Hindawi Publishing Corporation
Journal of Nanomaterials
Volume 2015, Article ID 549208, 8 pages
http://dx.doi.org/10.1155/2015/549208

Research Article

The Luminescence Properties and Energy Transfer from Ce^{3+} to Pr^{3+} for YAG:$Ce^{3+}Pr^{3+}$ Phosphors

Rongfeng Guan,[1] Liu Cao,[2] Yajun You,[1] and Yuebin Cao[1,3]

[1]*Key Laboratory for Advanced Technology in Environmental Protection of Jiangsu, Yancheng Institute of Technology, Jiangsu 224051, China*
[2]*Beijing Water Science Technology Institute, Beijing 100044, China*
[3]*Department of Chemical Engineering, Hanyang University, Ansan 426791, Republic of Korea*

Correspondence should be addressed to Yuebin Cao; hxxcyb@gmail.com

Received 25 March 2015; Revised 22 July 2015; Accepted 2 August 2015

Academic Editor: William W. Yu

$Y_{2.94-x}Al_5O_{12}$(YAG):$Ce_{0.06}Pr_x$ phosphors with various Pr^{3+} concentrations (x = 0, 0.006, 0.01, 0.03, 0.06, and 0.09) were synthesized by using a coprecipitation method. The phases, luminescent properties, and energy transfer phenomenon from Ce^{3+} to Pr^{3+} were investigated. The results indicated that the doping of Pr^{3+} ($x \leq 0.09$) did not produce any new phases but caused a slight lattice parameters increase. After Pr^{3+} doping, the YAG:CePr phosphor emits red light at 610 nm, which was regarded helpful for improving the colour rendering index of the phosphor. With Pr^{3+} concentration increase from 0.006 to 0.01 mol, the intensity of red light emission increased slightly; further increasing Pr^{3+} concentration from 0.01 to 0.09, the red light emission intensity decreased gradually. Excitation at 340, and 460 nm could not lead to the direct electronic excitation of Pr^{3+} ions; however, when YAG:CePr was excited at 340 nm a red light emission at 610 nm appeared, which implied the energy transfer phenomenon from Ce^{3+} to Pr^{3+}.

1. Introduction

As the fourth generation lighting sources, white-light emitting diodes (LEDs) have the following advantages: high efficiency to convert electrical energy to light, high reliability, and long operating lifetime (about 100000 h). They have been employed in the devices such as solid-state lasers, traffic lights, and field-emission displays [1–3]. Usually, white LEDs are fabricated by the combination of blue InGaN chips and yellow-emitting phosphor (YAG:Ce) [4–6]. However, the combined InGaN chips and YAG:Ce suffers from a low colour rendering index (<80) because of red light shortage in its emission spectrum. There are two methods to solve this problem: first, add an amount of red phosphor to yellow phosphor YAG:Ce to improve its colour rendering [7]; second, dope YAG:Ce phosphors to improve the red light emission [8–11]. As the ionic radius of Pr^{3+} is similar to Y^{3+}, it has been used to dope YAG:Ce phosphor to improve its red spectrum emission. Jang et al. [12] synthesized YAG:CePr phosphors with various Pr concentrations through a high temperature solid-state reaction. The obtained YAG:CePr phosphors used for white LEDs improved the colour rendering index between 80 and 83. Yang et al. [13] synthesized Pr^{3+} doped YAG:Ce nanopowder by polymer-assisted sol-gel method, which also showed a high colour rendering index of 83 in white LEDs. However, the researches on Pr^{3+} doped YAG:CePr are still limited; particularly, the energy transfer phenomenon from Ce^{3+} to Pr^{3+} is seldom researched. Here, we report the synthesis of YAG:CePr phosphors by a coprecipitation method, and the effects of Pr^{3+} doping concentrations on the properties of YAG:CePr including phases, light absorption, and luminescent properties are researched. In addition, the energy transfer from Ce^{3+} to Pr^{3+} is characterized and proved through luminescent and fluorescence lifetime measurements.

2. Experiments

YAG:$Ce_{0.06}Pr_x$ (x = 0, 0.006, 0.01, 0.03, 0.06, and 0.09) phosphors were prepared by coprecipitation method.

Stoichiometric amounts of source materials Y_2O_3(AR), $Al(NO_3)_3{\cdot}9H_2O$(AR), $Ce(NO_3)_3{\cdot}6H_2O$(AR), Pr_6O_{11}(AR), NH_4HCO_3(AR), $NH_3{\cdot}H_2O$(AR), and HNO_3(AR) were thoroughly mixed in solution. The Y^{3+} and Pr^{3+}/Pr^{4+} solution was obtained by dissolving Y_2O_3 and Pr_6O_{11} in HNO_3 aqueous solution, and this solution was denoted as solution A; $Al(NO_3)_3{\cdot}9H_2O$ and $Ce(NO_3)_3{\cdot}6H_2O$ were dissolved in a suitable amount of deionized water to obtain solution B; NH_4HCO_3 was also dissolved in deionized water, and the solution was denoted as C. Solutions A and B were mixed to obtain solution D, and then solution D was added (dropwise) to solution C at a rate of 1 mL/min. After finishing the dropping process, the system was adjusted to pH of 8 by using $NH_3{\cdot}H_2O$ and stirred for 2 h, and then the obtained precipitate was aged for 12 h. The white precipitate was filtered and then washed for 3 times by using deionized water and anhydrous ethanol, respectively. The filtered product was dried at 120°C for 12 h, ground, and mixed together with NaF (6 wt%) to form the precursor. The precursor was annealed at 1600°C for 3 h in a reductive atmosphere (with 95% N_2 and 5% H_2) to get the target product.

The phase characterization of the synthesised materials was conducted with X-ray powder diffraction (XRD) on a D8 Advance diffractometer (Bruker) operating at 40 kV, 200 mA, using Cu Kα radiation with a scanning rate of 1°/min and scanning range of $10^\circ \le 2\theta \le 80^\circ$.

The photoluminescence spectra were measured on powder samples at room temperature using Hitachi F-4500 luminescence spectrometer with a xenon discharge lamp (150 W) as the excitation source. The excitation spectra were obtained over the range of 200 to 550 nm and emission spectra were obtained over the range of 450 to 665 nm. Both excitation and emission splits were 5.0 nm, and the scanning interval was 0.2 nm. UV-visible absorption and diffuse reflectance spectra were monitored by a SHIMADAZU Japan UV 2700, with wavelength range from 200 to 800 nm and scanning interval of 0.5 nm.

3. Results and Discussion

3.1. Phases Analysis. Figure 1 shows XRD patterns of the YAG:$Ce_{0.06}Pr_x$ (x = 0, 0.006, 0.01, 0.03, 0.06, and 0.09) annealed at 1600°C for 3 h. All the diffraction peaks can be indexed to standard data of $Y_3Al_5O_{12}$ (JCPDS 33-0040), without the possible intermediate phases such as $Y_4Al_2O_9$ or $YAlO_3$. It means the samples were phase-pure and doping of the activator ions Pr^{3+} did not cause any observable new phases. Lattice parameters of YAG:$Ce_{0.06}Pr_x$ are calculated and the results are listed in Table 1. With increase of Pr^{3+} doping concentration, diffraction peaks of the phosphors shifted to lower degree and lattice parameters increased slightly, which can be explained by the larger radius of Pr^{3+} (r = 126.6 pm) than that of Y^{3+} (r = 115.9 pm).

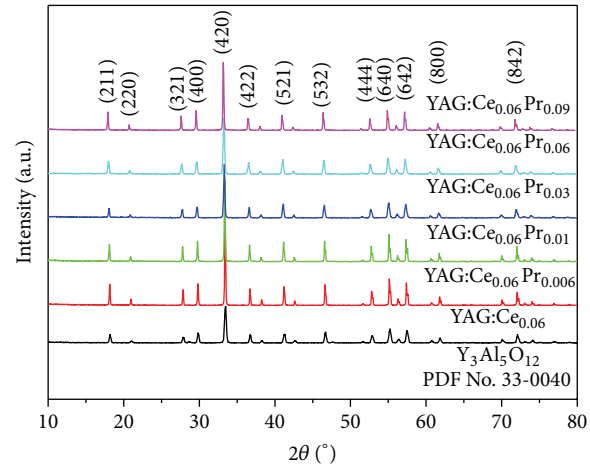

Figure 1: XRD patterns of YAG:$Ce_{0.06}Pr_x$ (x = 0, 0.006, 0.01, 0.03, 0.06, and 0.09) samples.

3.2. Spectral Analysis

3.2.1. Ultraviolet-Visible Absorption and Diffuse Reflectance Spectra. Figure 2(a) shows the absorption spectra of YAG:Ce. The excitation (absorption) peaks at 245, 340, and 457 nm were attributed to 4f → 5d transitions of the Ce^{3+} ions. The strong absorption peak located at 460 nm matched well with blue-light LED chips, which means the prepared YAG:Ce phosphors can absorb blue light from LED chips efficiently.

Figures 2(b)–2(e) show the absorption spectra of YAG:$Ce_{0.06}Pr_x$ phosphors with x = 0.01, 0.03, 0.06, and 0.09 mol, respectively. With increase of Pr^{3+} concentration, the two narrow absorption peaks appeared at 239 and 289 nm which correspond to the $4f^2(^3H_4) \rightarrow 4f5d$ transition of Pr^{3+} [9] increased significantly. When part Y^{3+} sites were substituted by Pr^{3+} ions, lattice parameters of the crystal became larger, causing subtle changes around the field of Ce^{3+} luminescence centre. Therefore, it is possible that the doping of Pr^{3+} will change absorption properties of Ce^{3+}. After Pr^{3+} doping, the typical absorption peaks of Ce^{3+} ions still exist in YAG:CePr phosphors, indicating the doping of Pr^{3+} has little effects on the absorption properties of Ce^{3+}. Presence of absorption peak at 457 nm means that YAG:CePr can absorb blue light from LED chips.

Diffuse reflection spectra of YAG:$Ce_{0.06}Pr_x$ were measured and the results were shown in Figure 3. YAG:Ce^{3+} phosphor without Pr^{3+} doping had a strong broad absorption peak at 460 nm and weak absorption band from 270 to 400 nm. With Pr^{3+} doping into the YAG:$Ce_{0.06}Pr_x$ phosphors, a small absorption peak appeared at 610 nm. With increase of Pr^{3+} concentration, intensity of the absorption peak at 610 nm gradually increased. At the same time, with Pr^{3+} concentration increase, the absorption intensity of 460 nm decreased, which may be caused by the formation of defects during Pr^{3+} doping [13].

3.2.2. Excitation and Emission Spectra. Figure 4 shows the emission spectra of YAG:$Ce_{0.06}Pr_x$ (x = 0.006, 0.01, 0.03, 0.06, and 0.09) phosphors excited at wavelengths of 340 nm and 460 nm, respectively. As shown in the emission spectra, they both show a broad peak around 534 nm and a sharp peak around 610 nm. The electron configuration of $4f^1$ for Ce^{3+} can transfer to its excited state of $4f^05d^1$ and split into

Table 1: Lattice parameters of YAG:$Ce_{0.06}Pr_x$ (x = 0, 0.006, 0.01, 0.03, 0.06, and 0.09).

YAG:$Ce_{0.06}Pr_x$	x = 0	x = 0.006	x = 0.01	x = 0.03	x = 0.06	x = 0.09
$a = b = c$ (Å)	11.9962	12.0105	12.0164	12.0190	12.0295	12.0327

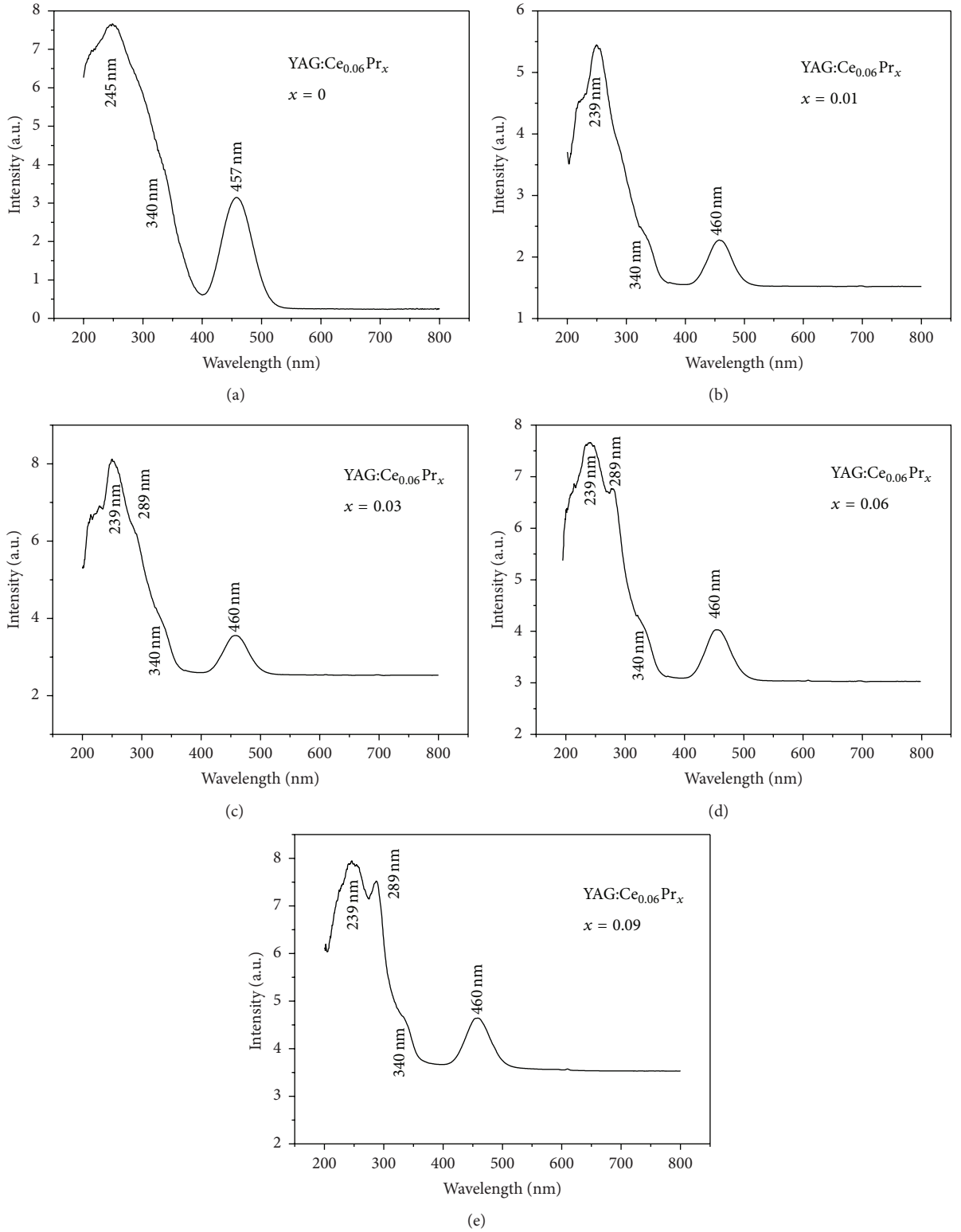

Figure 2: Absorption spectra of YAG:$Ce_{0.06}Pr_x$ phosphor with x = 0 (a), 0.01 (b), 0.03 (c), 0.06 (d), and 0.09 (e).

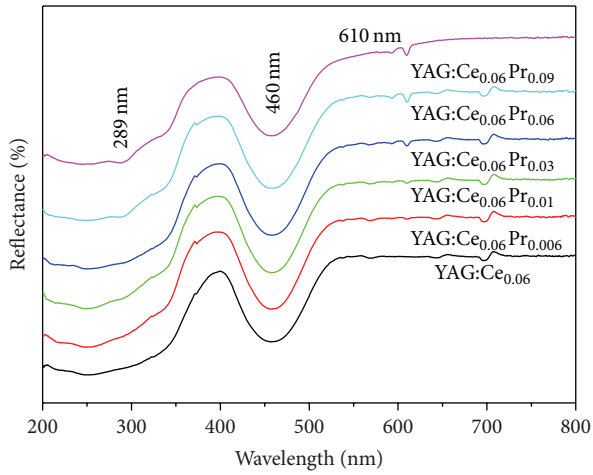

FIGURE 3: UV-vis diffuse reflectivity spectra of YAG:$Ce_{0.06}Pr_x$ phosphors.

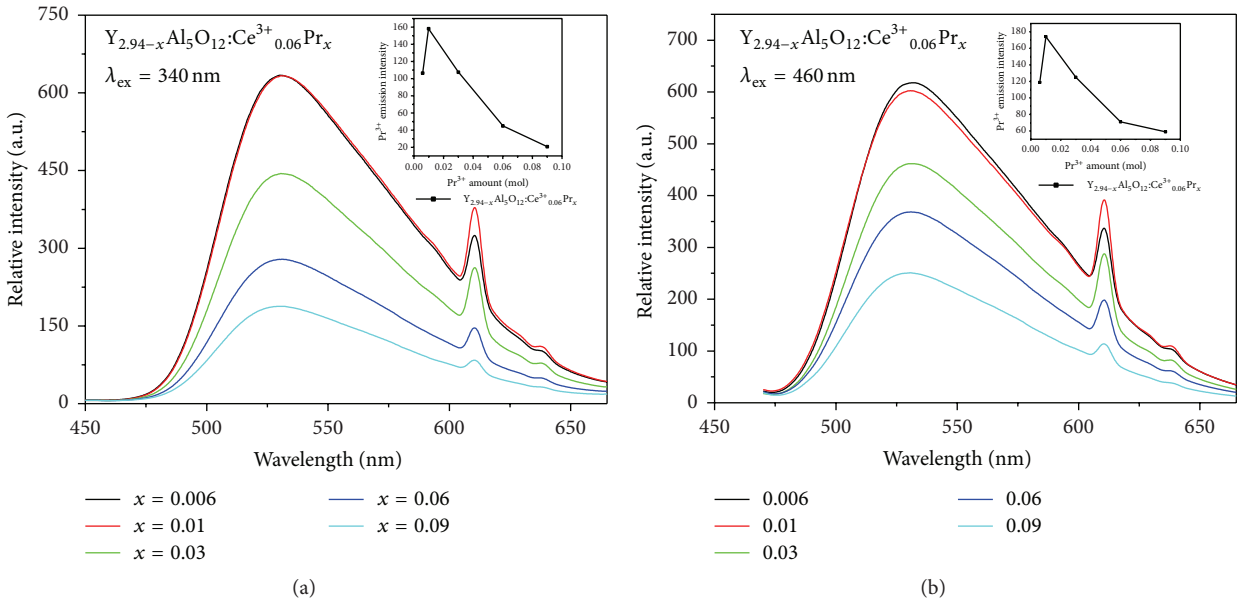

FIGURE 4: PL emission spectra of YAG:$Ce_{0.06}Pr_x$ phosphors excited at 340 nm (a) and 460 nm (b).

two spectroscopic terms $^2F_{7/2}$ and $^2F_{5/2}$ by spin coupling. The broad peak located at 534 nm in the yellow-green region can be attributed to the $4f^05d^1 \rightarrow {}^2F_{7/2}, {}^2F_{5/2}$ transition. The appearance of 610 nm, which is caused by $^1D_2 \rightarrow {}^3H_4$ transition of the Pr^{3+} ion [9, 13], indicates that Pr^{3+} doping increased the red light emission for YAG:$Ce_{0.06}Pr_x$. With Pr^{3+} doping concentration increasing, the intensity of yellow light emission at 534 nm decreased. Specifically, the intensity of the yellow light emission peak decreased from 632.48 ($x = 0.006$) to 183.24 ($x = 0.09$) under excitation at 340 nm (a decrease of 449.24); and the intensity decreased from 616.47 ($x = 0.006$) to 246.21 ($x = 0.09$) under excitation at 460 nm (a decrease of 370.26).

For the red light from Pr^{3+} emission at 610 nm, the intensity firstly increased to the maximum at $x = 0.01$ and then decreased monotonically. Insets of Figures 4(a) and 4(b) present the relation of the Pr^{3+} doping concentration and the PL emission intensity of 610 nm at excitation at 340 nm and 460 nm, respectively. Specifically, under excitation at 340 nm, the peak intensity increased gradually from 106.36 to 157.54 when x increased from 0.006 to 0.01 and then decreased from 157.54 to 21.16 when x further increased from 0.01 to 0.09. A similar trend for the spectra that are excited at 460 nm is shown. Firstly, with Pr^{3+} concentration increase (from 0.006 to 0.01), part Y^{3+} was substituted by Pr^{3+}, and thus intensity of red light which caused by Pr^{3+} increased. However, further increase of Pr^{3+} concentration (from 0.01 to 0.09) decreased the distance between Pr^{3+} and Pr^{3+}, which induced the self-quenching phenomenon, and thus decreased the light intensity.

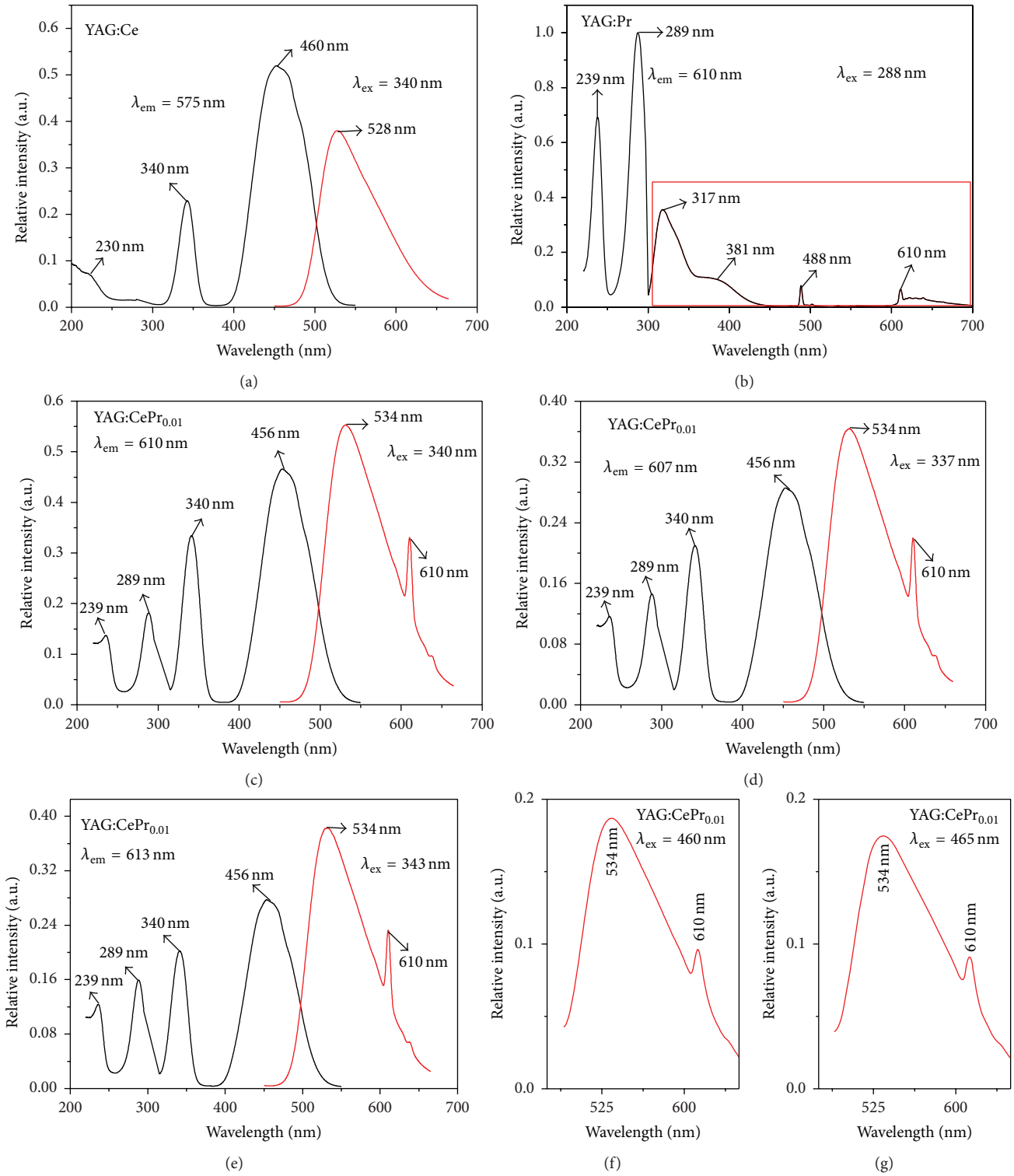

FIGURE 5: PL excitation and emission spectra of YAG:$Ce_{0.06}$ (a), YAG:$Pr_{0.01}$ (b), and YAG:$Ce_{0.06}Pr_{0.01}$ (c–g) (black line is excitation spectra, and red line is emission spectra. For Figure 6(b), the emission spectrum of YAG:$Pr_{0.01}$ was encircled with a red box).

Figure 5 shows the excitation and emission spectra of YAG:$Ce_{0.06}$, YAG:$Pr_{0.01}$, and YAG:$Ce_{0.06}Pr_{0.01}$, respectively. The sample with singly doped Ce^{3+} showed a strong yellow light emission at 528 nm arising from the 5d → 4f transitions of Ce^{3+} ions, and the excitation spectra included a blue absorption at 460 nm and two UV absorptions at 230 nm and 340 nm. For the singly doped Pr^{3+}, at an excitation at 288 nm, the emission spectra can be divided into three

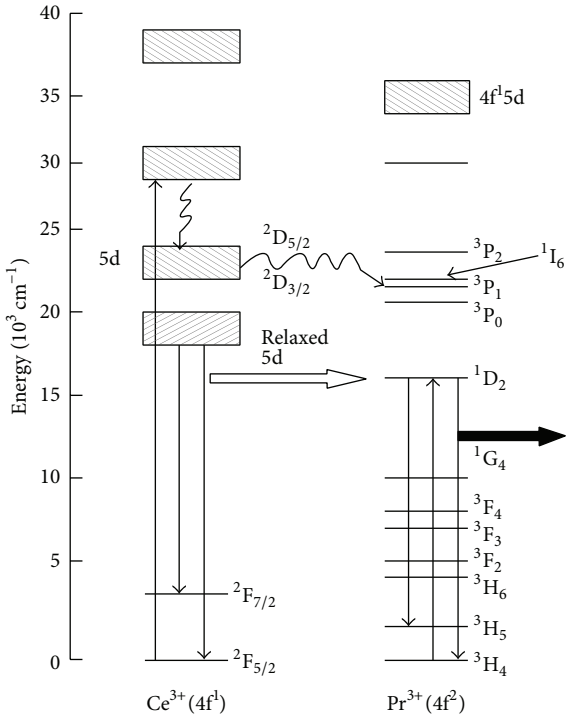

Figure 6: Energy level diagram and energy transfer of YAG:$Ce^{3+}Pr^{3+}$.

groups. The group in the UV region consisted of two broad emission bands at 317 nm and 381 nm, which were attributed to the 4f5d$\rightarrow {}^3H_J$ (J = 4, 5, and 6) and 4f5d$\rightarrow {}^3F_J$ (J = 2, 3, and 4) transitions of Pr^{3+}, respectively. The emission group in the range of 450 nm to 600 nm was attributed to the ${}^3P_0 \rightarrow {}^3H_{4,5}$ transition, and the main peak at 488 nm was due to ${}^3P_0 \rightarrow {}^3H_4$ transition. The other group was a red light emission at 610 nm, which was attributed to ${}^1D_2 \rightarrow {}^3H_4$ transitions. As shown in the excitation spectra of singly doped Pr^{3+}, two UV absorptions were located at 239 nm and 289 nm but no absorption peaks at 340 nm. However, under excitation at 340 nm, the emission spectra of Ce^{3+} and Pr^{3+} codoped YAG:$Ce_{0.06}Pr_{0.01}$ exhibit not only the yellow emission caused by Ce^{3+} but also the red emission caused by Pr^{3+} (Figure 5(c)). Figures 5(d) and 5(e) show the emission spectra excited at 337 nm and 343 nm respectively, and they also show similar emission spectra to that excited at 340 nm. As the excitation at 340 nm cannot lead to the direct electronic excitation of Pr^{3+} ions, the appearance of 610 nm red line emission from Pr^{3+} indicates the energy transfer from the excited Ce^{3+} to its neighbouring Pr^{3+} ions. To further prove the energy transfer phenomenon, YAG:$Ce_{0.06}Pr_{0.01}$ was excited at 460 and 465 nm, and its emission spectra were shown in Figures 5(f) and 5(g). It can be seen that the red light emission at 610 nm also exists under excitation at 460 and 465 nm, which further confirmed the energy transfer from Ce^{3+} to Pr^{3+}.

Figure 6 shows the energy level diagram and energy transfer behaviour of YAG:$Ce^{3+}Pr^{3+}$. It shows that the energy can be transferred from the 5d relaxed state of Ce^{3+} ion to ${}^1D_2$ energy level of the Pr^{3+} ion through a radiative transition process. And the energy can also be transferred from the lowest 5d band of Ce^{3+} to ${}^3P_0$ energy level of Pr^{3+} through a nonradiative process. The relaxed lowest 5d band of the Ce^{3+} ion is located at around 18,500 cm^{-1}, and therefore the energy transfer may occur radioactively at the D single state and the ${}^1D_2 \rightarrow {}^3H_4$ transition may lead to red light emission. If the energy transfers from the 5d energy band of Ce^{3+} to the ${}^3P_0$ energy band of Pr^{3+} through a nonradiative transition, a green light emission (${}^3P_0 \rightarrow {}^3H_4$) and a red light emission (${}^1D_2 \rightarrow {}^3H_4$) should appear simultaneously. However, the green light emission (${}^3P_0 \rightarrow {}^3H_4$) did not appear which meant that the nonradiative transition from the lowest 5d band of Ce^{3+} to ${}^3P_0$ energy level of Pr^{3+} did not happen [9]. As shown in the above emission spectra, there was only a weak red emission (610 nm) due to the ${}^1D_2 \rightarrow {}^3H_4$ transition of Pr^{3+}, indicating the existence of radiative energy transfer from the 5d relaxed state of Ce^{3+} to the ${}^1D_2$ energy level of Pr^{3+}.

3.2.3. Fluorescence Lifetime. The fluorescence decay curves of the samples were measured, and they were exponentially fitted to obtain the fluorescence decay lifetime [14]. Figures 7(a) and 7(b) show the decay curves of yellow light emission under excitation at 340 and 460 nm, which were monitored at 534 nm. Figure 7(c) shows the decay curves of the red emission for the ${}^1D_2 \rightarrow {}^3H_5$ transition of Pr^{3+} under excitation at 340 nm, which were monitored at 610 nm. The fluorescence lifetimes of Ce^{3+} and Pr^{3+} are listed in Table 2. When doping Pr^{3+} into YAG:Ce^{3+}, the lifetime of yellow light

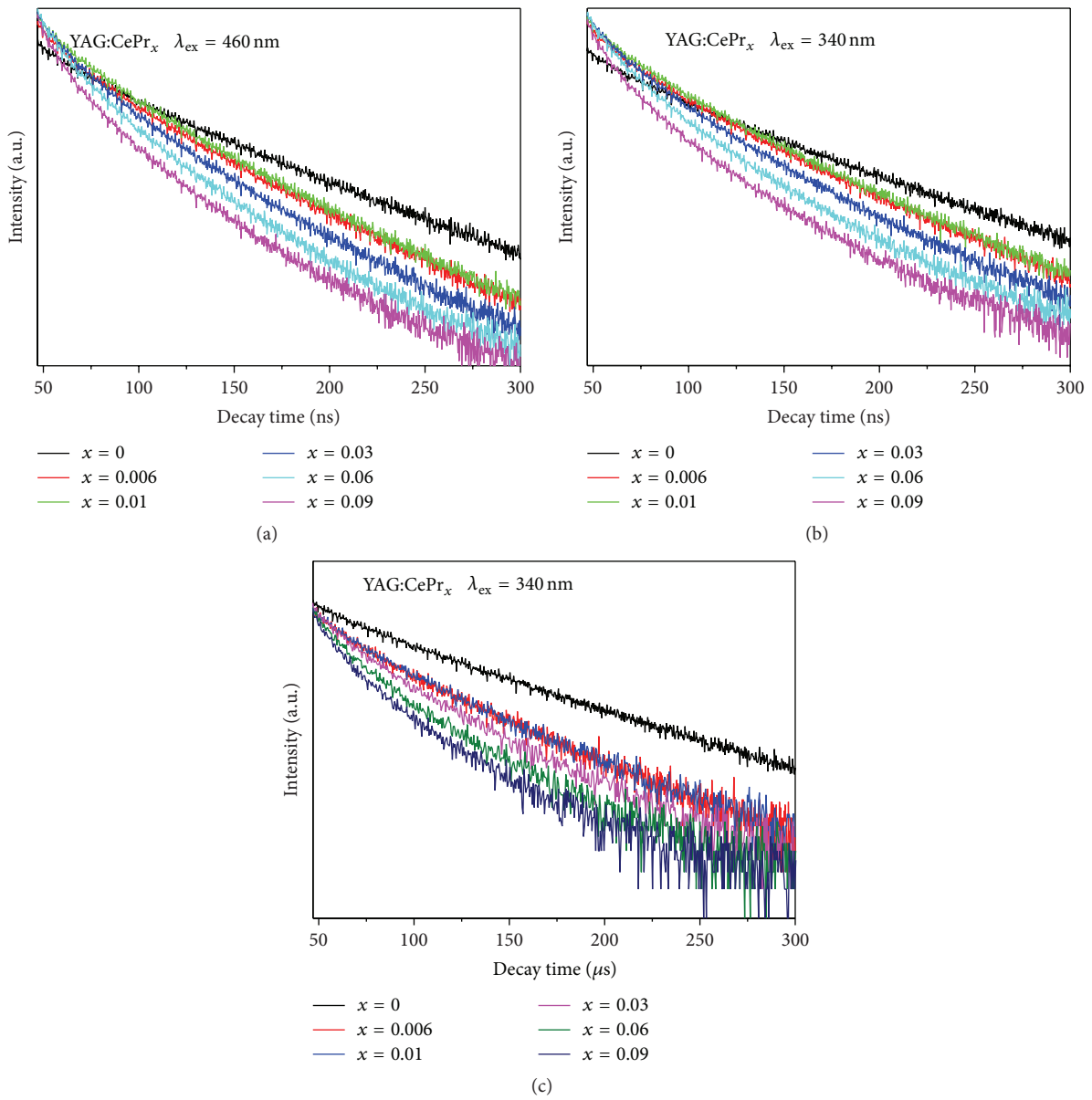

Figure 7: (a, b) Fluorescence lifetime of yellow light (534 nm) excited at wavelengths 340 nm (a) and 460 nm (b). (c) Fluorescence lifetime of red light (610 nm) excited at wavelength 340 nm.

decreased, and it further decreased as Pr^{3+} concentrations increase. Specifically, at excitation at 340 nm, fluorescence lifetimes of the yellow light emission decreased from 34.6 ns to 7.5 ns; and at excitation at 460 nm the fluorescence lifetimes decreased from 35.6 ns to 7.3 ns. In YAG:Ce^{3+}, only the energy transfer between two Ce^{3+} can happen, while in the codoped YAG:$Ce^{3+}Pr^{3+}$ there can be energy transfer between Pr^{3+} and Ce^{3+}. It may be the reason for lifetime decrease of yellow light. In the case of energy transfer from Ce^{3+} to Pr^{3+}, the decrease time from Ce^{3+} should be equal to the rise time from Pr^{3+}. However, the rise time from Pr^{3+} was not found here; oppositely, the lifetime of red light also decreased with Pr^{3+} doping. We guess the self-quenching between Pr^{3+} and Pr^{3+} maybe caused the lifetime decrease of red light.

4. Conclusions

A series of YAG:$Ce_{0.06}Pr_x$ phosphors with various Pr^{3+} concentrations (x = 0, 0.006, 0.01, 0.03, 0.06, and 0.09) were synthesised by coprecipitation method. Doping of Pr^{3+} did not change the phase of the YAG but induced a slight lattice parameters increase. Under excitation at either 340 nm or 460 nm, they both show a broad emission peak at 534 nm and a narrow emission peak at 610 nm. Appearance of the red emission peak at 610 nm was beneficial for improving the colour rendering of YAG:Ce^{3+}. As Pr^{3+} concentration increased from 0.006 to 0.01 mol, the intensity of red light emission increased slightly, and then it decreased gradually when Pr^{3+} concentration further increased from 0.01 to 0.09.

Table 2: Fluorescence lifetime of yellow and red light in $Y_{2.94-x}Al_5O_{12}:Ce^{3+}{}_{0.06}Pr_x$.

x	τ (ns) 5d of Ce^{3+}		τ (μs) $^1D_2$ of Pr^{3+}
	λ_{ex} = 340 nm λ_{em} = 534 nm	λ_{ex} = 460 nm λ_{em} = 534 nm	λ_{ex} = 340 nm λ_{em} = 610 nm
0	34.6	35.6	28.5
0.006	16.7	16.8	19.4
0.01	15.6	15.7	16.7
0.03	11.8	12.0	15.1
0.06	9.0	9.5	9.7
0.09	7.5	7.3	8.3

Emission properties of YAG:CePr at excitation at 340 and 460 nm proved the energy transfer from Ce^{3+} to Pr^{3+}.

Conflict of Interests

The authors declare that there is no conflict of interests regarding the publication of this paper.

Acknowledgments

This work was financially supported by the National Natural Science Foundation (Grant no. 21276220), the National Key Technology Support Programme (Grant no. 2013BAC13B00), Yancheng Institute Of Technology Talent Programme (Grant no. KJC2013007), and Jiangsu Province Qing Lan Project and The Key Laboratory for Advanced Technology in Environmental Protection of Jiangsu Province (Grant no. AE201124).

References

[1] H. S. Jang, Y.-H. Won, and D. Y. Jeon, "Improvement of electroluminescent property of blue LED coated with highly luminescent yellow-emitting phosphors," *Applied Physics B: Lasers and Optics*, vol. 95, no. 4, pp. 715–720, 2009.

[2] J. K. Kim and E. F. Schubert, "Transcending the replacement paradigm of solid-state lighting," *Optics Express*, vol. 16, no. 26, pp. 21835–21842, 2008.

[3] F. K. Yam and Z. Hassan, "Innovative advances in LED technology," *Microelectronics Journal*, vol. 36, no. 2, pp. 129–137, 2005.

[4] R. Michael, O. Krames, B. Shchekin, M. M. Regina, G. O. Mueller, and L. Zhou, "Status and future of high-power light-emitting diodes for solid-state lighting," *Journal of Display Technology*, vol. 3, pp. 160–175, 2007.

[5] S. Ye, F. Xiao, Y. X. Pan, Y. Y. Ma, and Q. Y. Zhang, "Phosphors in phosphor-converted white light-emitting diodes: recent advances in materials, techniques and properties," *Materials Science and Engineering R: Reports*, vol. 71, no. 1, pp. 1–34, 2010.

[6] H.-T. Huang, Y.-P. Huang, and C.-C. Tsai, "Planar lighting system using array of blue leds to excite yellow remote phosphor film," *IEEE/OSA Journal of Display Technology*, vol. 7, no. 1, pp. 44–51, 2011.

[7] Z. Y. Liu, S. Liu, K. Wang, and X. B. Luo, "Optical analysis of phosphor's location for high-power light-emitting diodes," *IEEE Transactions on Device and Materials Reliability*, vol. 9, no. 1, pp. 65–73, 2009.

[8] C. C. Lin and R.-S. Liu, "Advances in phosphors for light-emitting diodes," *The Journal of Physical Chemistry Letters*, vol. 2, no. 11, pp. 1268–1277, 2011.

[9] X. Zhou, K. Zhou, Y. Li, Z. Wang, and Q. Feng, "Luminescent properties and energy transfer of $Y_3Al_5O_{12}:Ce^{3+},Ln^{3+}$ (Ln=Tb, Pr) prepared by polymer-assisted sol-gel method," *Journal of Luminescence*, vol. 132, no. 11, pp. 3004–3009, 2012.

[10] W. Wang, J. Tang, and P. Sullivan, "Energy transfer and enriched emission spectrum in Cr and Ce co-doped $Y_3Al_5O_{12}$ yellow phosphors," *Chemical Physics Letters*, vol. 457, pp. 103–105, 2008.

[11] H. Yang and Y.-S. Kim, "Energy transfer-based spectral properties of Tb-, Pr-, or Sm-codoped YAG:Ce nanocrystalline phosphors," *Journal of Luminescence*, vol. 128, no. 10, pp. 1570–1576, 2008.

[12] H. S. Jang, W. B. Im, D. C. Lee, D. Y. Jeon, and S. S. Kim, "Enhancement of red spectral emission intensity of $Y_3Al_5O_{12}:Ce^{3+}$ phosphor via Pr co-doping and Tb substitution for the application to white LEDs," *Journal of Luminescence*, vol. 126, no. 2, pp. 371–377, 2007.

[13] H. Yang, D.-K. Lee, and Y.-S. Kim, "Spectral variations of nano-sized $Y_3Al_5O_{12}$:Ce phosphors via co-doping/substitution and their white LED characteristics," *Materials Chemistry and Physics*, vol. 114, no. 2-3, pp. 665–669, 2009.

[14] R. Singh and B. Pal, "Study of excited charge carrier's lifetime for the observed photoluminescence and photocatalytic activity of CdS nanostructures of different shapes," *Journal of Molecular Catalysis A: Chemical*, vol. 371, pp. 77–85, 2013.